ISSN 2176-5480

22nd International Congress of Mechanical Engineering (COBEM 2013)
November 3-7, 2013, Ribeirão Preto, SP, Brazil

PREDICTION OF TEMPERATURE DISTRIBUTION IN INDUCTION MOTORS OF RECIPROCATING COMPRESSORS

Thiago Dutra
Cesar J. Deschamps
Federal University of Santa Catarina, Florianópolis, Brazil
dutra@polo.ufsc.br, deschamps@polo.ufsc.br

Abstract. *The temperature distribution of induction motors is an important aspect required to assess the efficiency and reliability of refrigeration compressors. The present paper details a steady state thermal model developed to predict the temperature of different components of an induction motor. Such a model is based on a lumped-parameter formulation of the energy equation and adopts temperature measurements in the motor surroundings as boundary conditions. Additionally, a single-phase electrical motor equivalent circuit is adopted to predict motor losses that are used as input data in the thermal model. Both models are solved in a coupled manner, since the motor electric resistances are affected by temperature, and vice-versa.*

Keywords: *thermal management, induction motors, reciprocating compressors.*

1. INTRODUCTION

Efficiency and reliability of induction motors are affected by their thermal profiles. In the case of motors of low efficiency, a considerable part of the energy input is converted into heat and this rises up the temperature of the motor components. The electrical motor may fail when the operating temperature exceeds the temperature limit specified for different components. Due to these issues, thermal management of induction motors is a key aspect to be considered in the design stage. This is even more critical for refrigeration compressors because its thermal profile impacts not only the electrical motor but also the compressor thermodynamic efficiency.

Several papers about thermal modeling of induction motors are available in literature. The lumped-parameter methodology (Mellor *et al.,* 1991; Eltom and Moharari, 1991; Umans, 1996; Voigdlener, 2004; Chowdhury, 2005; Mezani *et al.*, 2005; Eme *et al.*, 2006) and the finite element methodology (Hwang *et al.*, 1997; Rajagopal *et al.*, 1998; Huai *et al.*, 2003; Sarkar and Naskar, 2012) are the most used approaches.

The lumped-parameter methodology considers a division of the motor geometry into a number of lumped isothermal components and the energy equation applied to each one of them. The lumped element temperature is then obtained as the solution of the equation system. The interconnection among neighbor elements is accomplished by thermal conductances, which are modeled by equivalent thermal resistances. The lumped-parameter formulation is usually associated with low computational cost.

The finite-element methodology (FEM) adopts a more refined division of the computational domain and is usually employed in situations where a more detailed analysis is required, such as the determination of the thermal gradient in components. Since FEM is characterized by a large number of elements, the higher accuracy level comes at the expense of higher computational cost when compared to the lumped formulation.

Regardless the formulation employed, it is necessary to prescribe reliable boundary conditions for the thermal model. In this context, heat generation rate due to the electrical losses distribution inside the induction motor is a very important aspect. Such losses can be experimentally obtained and prescribed in the computational model. However, a great part of the electrical losses may also be computed from electrical motor models. Indeed, most simulation models in the literature (Mellor *et al.,* 1991; Eltom and Moharari, 1991; Umans, 1996; Huai *et al.*, 2003; Mezani *et al.*, 2005) adopt thermo-electrical models in which the thermal and electrical models are coupled to each other.

Thermal modeling of refrigeration compressors is also a topic frequently reported in literature. Likewise in induction motors, thermal models of compressors are developed using different formulations. The lumped-parameter methodologies are well disseminated and some use experimental data (Todescat *et al.*, 1992) whilst others use empirical correlations from literature (Padhy, 1992; Ooi, 2003) to establish thermal conductances. The finite volume methodology (FVM) is also largely employed (Raja *et al.*, 2003; Bivari *et al.*, 2006; Schreiner, 2008) with fluid flow and heat transfer equations being solved without requiring conductances. Most models based on FVM solve the Navier-Stokes equations and, therefore, are computationally expensive. Due to that, hybrid models have been developed (Schreiner, 2008; Sanvezzo, 2012) so that lumped formulation can be adopted for fluid elements, whereas FVM is only required in solid elements. The induction motor losses required as input for compressor thermal models are prescribed from established relations between the motor electrical efficiency and its power consumption, usually obtained from dynamometer tests.

The present paper reports the development of a simplified thermo-electrical model to predict the temperature profile of an induction motor adopted in small refrigeration reciprocating compressors. The compressor induction motor is single-phase and operates with no run-capacitor. This type of motor has a stator built with main and auxiliary copper

ISSN 2176-5480

windings, but the latter is used only to start up. The steady state condition is established with main winding and this allows a simple electrical modeling based on the motor equivalent circuit. The thermal model employs a lumped-parameter formulation. Predictions are compared to experimental data under different operating conditions and reasonable agreement is observed.

2. THERMAL MODEL

As depicted in Fig. 1, the motor geometry was divided into general cylindrical elements and a 2-D approach was used to model the conductive thermal resistances. Such an approach is very similar to that adopted by Voigdlener (2004) and considers the thermal resistances to be axial or radial, assuming no circumferential heat transfer.

The first law of thermodynamics applied to a generic lumped element "*i*" gives:

$$\dot{Q}_i + \sum_{j=1}^{n} \dot{m}_{j,i} h_{j,i} = \dot{W}_i + \sum_{k=1}^{m} \dot{m}_{i,k} h_{i,k} + \frac{d(m_i u_i)}{dt} \tag{1}$$

where $\dot{Q}_i$ (W) is the convective/conductive heat transfer rate between *i* and vicinity, $\dot{W}_i$ (W) is the mechanical power acting on the element boundaries, $\dot{m}_{j,i} h_{j,i}$ and $\dot{m}_{i,k} h_{i,k}$ (W) are the advective heat transfer that come from the element *j* towards *i*, and leave element *i* towards *k*, respectively. The thermal storage term is represented by $d(m_i u_i)/dt$ (W). In the present paper, a steady state formulation is considered, with no advective heat transfer between elements and no expansion/contraction of elements. Accordingly, Eq. (1) is simplified to:

$$\dot{Q}_i = 0 \tag{2}$$

and $\dot{Q}_i$ is modeled as the summation of heat transfer portions between element *i* and each neighbor *j* plus the internal heat generation of element *i*. The heat transfer portions can be written as a combination of temperature difference and thermal conductance between elements. Thus,

$$\sum_{j=1}^{n} H_{i,j} \left(T_i - T_j\right) - \dot{S}_i = 0 \tag{3}$$

where $H_{i,j}$ (W.K^{-1}) is thermal conductance, T (K) is temperature and $\dot{S}_i$ (W) is the source term, used to prescribe local heat generation and boundary conditions. The thermal conductance is the inverse function of equivalent thermal resistance, $R_{i,j}^{eq}$ (K.W^{-1}):

$$R_{i,j}^{eq} = \frac{\left(T_i - T_j\right)}{\dot{Q}_{ij}} \tag{4}$$

The equivalent thermal resistances are computed from combining conductive and convective resistances between thermal lumped elements, since radiation heat transfer is neglected. The conductive thermal resistances are modeled as:

$$R^a = \frac{L}{\lambda S_{cs}} \tag{5}$$

and

$$R^r = \frac{\ln(r_{ext}/r_{int})}{4\pi\lambda L} \tag{6}$$

where L (m) is the distance between the lumped node, placed at the geometrical center of the element, and the axial boundary, λ (W.m^{-1}.K^{-1}) is the thermal conductivity of the material, S_{cs} (m^2) is the cross sectional area of the lumped element and r_{ext} and r_{int} (m) are the external and internal radii of the element. Convective thermal resistance is given by:

$$C = \frac{1}{hS} \tag{7}$$

where h (W.m^{-2}.K^{-1}) is the convective heat transfer coefficient and S (m²) is the element surface area exposed to convection heat transfer. The convective coefficient is obtained from the definition of Nusselt number, *Nu* (-):

ISSN 2176-5480

$$h = \frac{Nu_{Lc}\lambda_f}{Lc} \tag{8}$$

where λ_f is the thermal conductivity of the fluid, L_c (m) is the characteristic length and Nu_{Lc} is obtained from empirical correlations available in literature and will be shown in the next section. Since thermal resistances and heat generation rates are calculated, Eq. (3) may be rearranged in a matrix form:

$$\sum_{j=1}^{n} A_{i,j} T_j = B_i \tag{9}$$

where $A_{i,j}$ is the thermal conductances matrix and B_i is the heat generation vector. Equation (9) is written for each of the 43 elements of the electrical motor and the iterative Newton-Raphson method is employed to solve the linear system. Figure 2 shows a schematic of the thermal circuit. The heat generation nodes are surrounded by a circular dashed line.

In order to illustrate the application of the thermal model, the energy balance is described for lumped element 4, which is the upper part of the crankshaft. This element is surrounded by crankcase (1), lubricant oil flow (3) and the intermediate part of the crankcase (5). Thus,

$$\left(H_{4,1} + H_{4,3} + H_{4,5}\right)T_4 - H_{4,1}T_1 - H_{4,3}T_3 - H_{4,5}T_5 = 0 \tag{10}$$

and the thermal conductances are:

$$H_{4,1} = \left(R_{4,1}^{eq}\right)^{-1} = \left(R_{4,1}^{a}\right)^{-1} + \left(R_{4,1}^{r}\right)^{-1}; \qquad H_{4,3} = \left(R_{4,3}^{eq}\right)^{-1} = \left(R_{4,3}^{r} + C_{4,3}^{r}\right)^{-1};$$
$$H_{4,5} = \left(R_{4,5}^{eq}\right)^{-1} = \left(R_{4,5}^{a} + R_{5,4}^{a}\right)^{-1} \tag{11}$$

The thermal resistances are calculated as:

$$R_{4,1}^{a} = L_{4,1}/\lambda_4 A_{4,1}\,; \qquad R_{4,3}^{r} = \ln(D_{inter\,4}/D_{int\,4})/4\pi\lambda_4 L_{4,1}\,; \qquad R_{4,1}^{r} = \ln(D_{ext\,4}/D_{inter\,4})/4\pi\lambda_4 L_{4,1}\,;$$
$$R_{4,5}^{a} = L_{4,5}/\lambda_4 A_{4,5}\,; \qquad R_{5,4}^{a} = L_{5,4}/\lambda_5 A_{5,4}\,; \qquad C_{4,3}^{r} = 1/h_{4,3}A_{4,3} \tag{12}$$

the diameters D_{ext4}, D_{inter4} and D_{int4}(m) correspond to external, internal and intermediate diameters of element 4, respectively. The node of the lumped element is positioned on the intermediate diameter, which is derived from a combination of the internal and external diameters:

$$D_{inter\,4} = \sqrt{\frac{{D_{int\,4}}^2 + {D_{ext\,4}}^2}{2}} \tag{13}$$

Equation (10) is rewritten in a matrix form:

$$A_{4,4}T_4 + A_{4,1}T_1 + A_{4,3}T_3 + A_{4,5}T_5 = 0 \tag{14}$$

and

$$A_{4,4} = H_{4,1} + H_{4,3} + H_{4,5}; \qquad A_{4,1} = -H_{4,1}; \qquad A_{4,3} = -H_{4,3}; \qquad A_{4,5} = -H_{4,5}; \qquad B_4 = 0 \tag{15}$$

2.1 Convective heat transfer coefficients

The convective heat transfer coefficients were obtained from correlations available in literature:

1. *Between lubricant oil flow (3)and crankshaft (4, 5) or oil pump (8,9):*Since there is a helical channel machined in the crankshaft and the lubricant oil flows inside this channel, the correlation proposed by Janssen and Hoogendoorn (1978) was used to calculate the Nusselt number:

$$Nu = \left(\frac{0.32 + 3\,d/D}{0.86 - 0.8\,d/D}\right) Re_d^{0.5} Pr^{0.33} (d/l)^{0.14 + 0.8\,d/D} \tag{16}$$

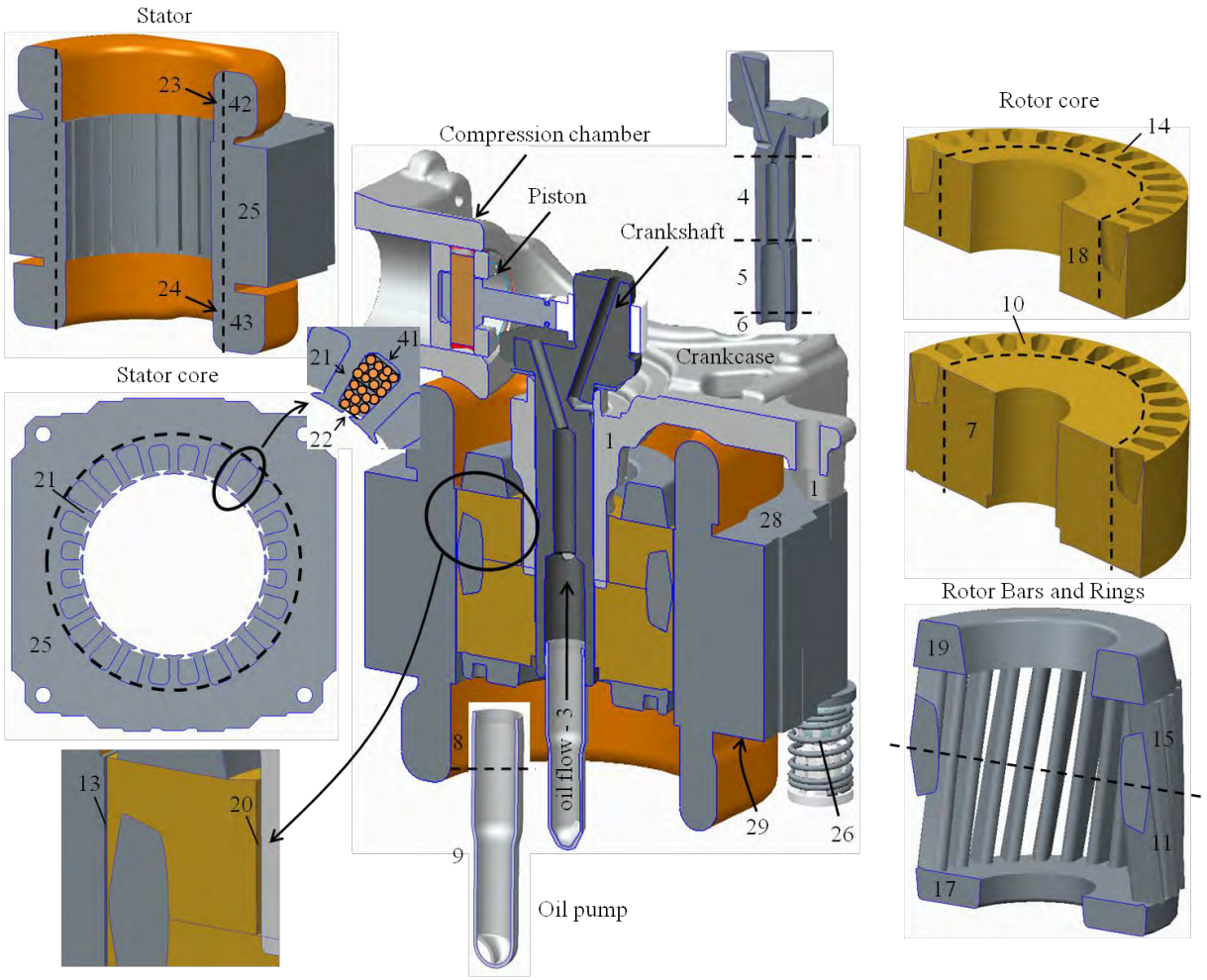

Figure 1. Electrical motor geometry.

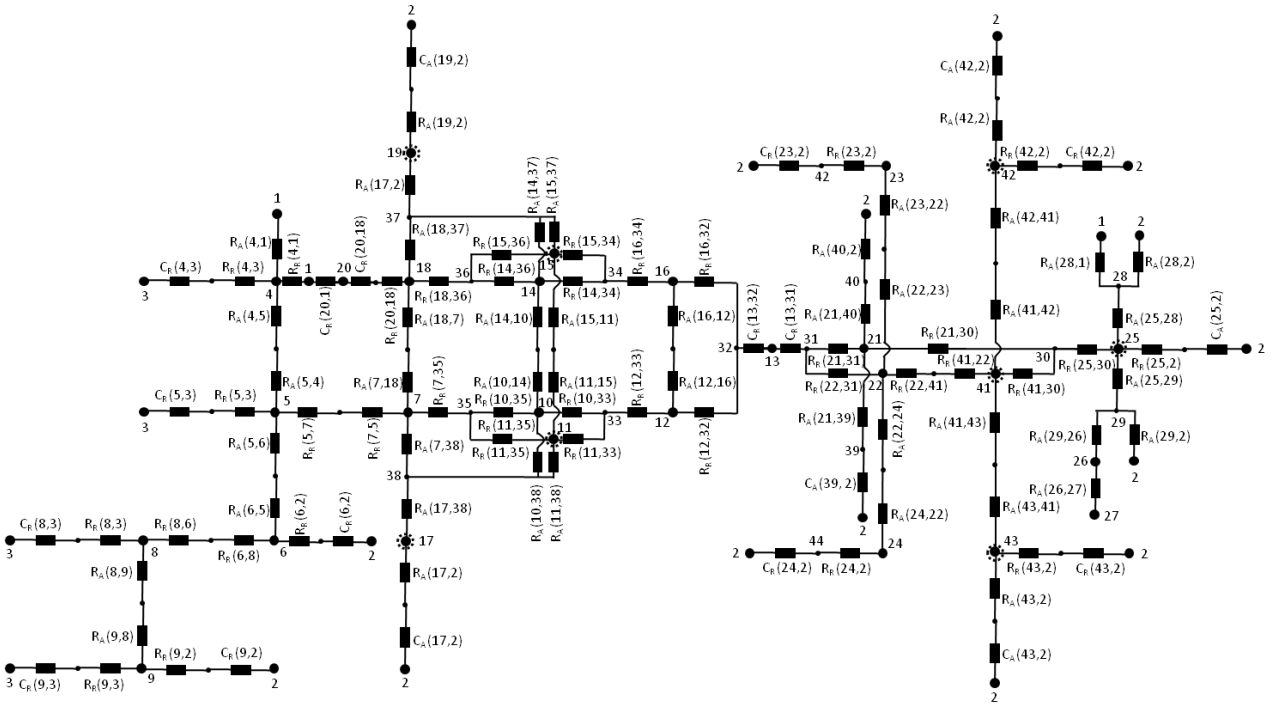

Figure 2. Electrical motor thermal circuit.

ISSN 2176-5480

where *Pr* is the Prandtl number, *l* is the channel length, and *d* and *D* are the channel and shaft diameters, respectively. The Reynolds number, Re_d, adopts the channel diameter, *d*, as the characteristic length:

$$Re_d = \frac{4Q}{\pi d \nu} \tag{17}$$

where *Q* ($m^3.s^{-1}$) is the oil volumetric flow rate through the channel and was assumed to be 0.8 x 10^{-3} $m^3.s^{-1}$, based on data supplied by the compressor manufacturer. An overall heat transfer coefficient is adopted along the crankshaft and oil pump.

2. *Between crankshaft (6) and refrigerant gas inside the compressor (2)*: The convection heat transfer between a small portion of the crankshaft (6) and the refrigerant gas (2) is modeled with the correlation of Whitaker (1972), which was obtained for a rotating cylinder:

$$Nu = 0.133 Re_D^{0.67} Pr^{0.33} \tag{18}$$

where Re_D is calculated using the external crankshaft diameter.

3. *Between oil pump (9) and refrigerant gas inside the compressor (2)*: The correlation of Whitaker (1972) was also used to model the convection heat transfer between the rotating oil pump and the refrigerant gas.

4. *Between rotor aluminum rings (17, 19) and refrigerant gas inside the compressor (2)*: The rotor rings are assumed as rotating discs and the correlation proposed by Cobb and Saunders (1959) was adopted to model the convective heat transfer:

$$Nu = 0.016 Re_r^{0.8} Pr^{0.33} r^{0.8} \tag{19}$$

where *r* is the disc radius and corresponds to the ring external radius.

6. *Between air-gap (13) and rotor (32) or stator (31)*: The correlation obtained by Bouafia *et al.* (1998) was used. The authors proposed a convective heat transfer correlation in an annular gap delimited by internal rotating and external stationary cylinders, which is very similar to the current one.

$$Nu = 0.132 Ta_{gap}^{0.3} \quad \text{for} \quad 6000 < Ta_{gap} < 1.4 \text{ x } 10^6 \tag{20}$$

$$Nu = 0.029 Ta_{gap}^{0.4} \quad \text{for} \quad 1.4 \text{ x } 10^6 < Ta_{gap} < 2 \text{ x } 10^7 \tag{21}$$

where Ta_{gap} is a non-dimensional parameter used to analyze fluid flows in small annular gaps and is defined as:

$$Ta_{gap} = \frac{\omega^2 r_m gap^3}{\nu^2} \tag{22}$$

where ω (rad.s^{-1}) is the angular velocity, *gap* is the difference between stator internal (r_{int}^{sta}) and rotor external (r_{ext}^{rot}) radii, and r_m is the logarithmic average radius:

$$r_m = gap / \ln(r_{ext}^{rot} / r_{int}^{sta}) \tag{23}$$

7. *Between rotor-crankcase gap (20) and rotor (18) or crankcase (1)*: This situation considers a convective heat transfer in a small gap between cylindrical stationary and rotating surfaces, then the correlation of Bouafia *et al.* (1998) was employed. Since such a components arrangement is not identical to Bouafia *et al.* (1998), a sensitivity analysis was carried out to estimate the influence of this convective heat transfer coefficient on the motor thermal profile. Even when Bouafia *et al.* (1998) correlation is multiplied by factors 0.2 and 5, temperature maximum variation is lower than 0.1 K. Therefore, the heat transfer modeling in this specific location was assumed to be not critical.

8. *Between stator iron horizontal surfaces (28, 29) and refrigerant gas inside the compressor (2)*: The correlations for natural convection on hot horizontal plates are used (Incropera and DeWitt, 2011). For a top surface of a hot plate (28):

$$Nu = 0.54 Ra_L^{0.25} \quad \text{for} \quad 10^4 < Ra_L < 10^7 \tag{24}$$

$$Nu = 0.15 Ra_L^{0.33} \quad \text{for} \quad 10^7 < Ra_L < 10^{11} \tag{25}$$

ISSN 2176-5480

and for a bottom surface of a hot plate (29):

$$Nu = 0.27Ra_L^{0.25} \qquad \text{for} \qquad 10^5 < Ra_L < 10^{10} \tag{26}$$

where Ra_L is the Rayleigh number and represents a non-dimensional parameter used to evaluate the intensity of natural convection. This number is defined as:

$$Ra_L = \frac{g\beta(T_s - T_f)L^3}{\nu\alpha} \tag{27}$$

where g (m.s^{-2}) is gravity acceleration, β (K^{-1}) is fluid thermal expansion coefficient, T_s and T_f are temperatures of surface and fluid, respectively. The characteristic length, L, is defined as a relation between horizontal surface area and plate perimeter ($L = A/P$).

9. *Between stator copper coils (23, 24, 42, 43) and refrigerant gas inside the compressor (2)*: Auxiliary winding (22, 23 and 24) are modeled as being closer to the rotor than main winding (41, 42 and 43). Therefore, the coil elements 23 and 24 are exposed to a forced convection generated by the crankshaft/rotor assembly rotation. The correlation regarding forced convection over a flat plate was used (Incropera and DeWitt, 2011):

$$Nu = 0.037Re_L^{0.8}Pr^{0.33} \tag{28}$$

where L is the internal perimeter of the auxiliary coil. The main coil elements 41 and 43 may be assumed to be exposed to natural convection. Their radial boundaries are considered as vertical flat plates, thus the correlation of Churchill and Chu (1975) is adopted:

$$Nu = \left\{0.825 + \frac{0.387Ra_L^{0.25}}{[1 + (0.492/Pr)^{0.56}]^{0.44}}\right\}^2 \tag{29}$$

and the axial boundaries are considered as horizontal plate, then hot horizontal plate correlations are used (Eqs. 24-26).

10. *Between stator iron (25) and refrigerant gas inside the compressor (2)*: The vertical surface of the stator iron is a vertical flat plate submitted to natural convection. Then, the correlation of Churchill and Chu (1975) was employed.

3. ELECTRICAL MODEL

The electrical model was based on a classical approach known as Equivalent Circuit Methodology. This technique consists on representing the electrical motor in an equivalent circuit using a set of stator (1), rotor (2) and magnetizing (m) impedances (Hrabovcova *et al.*, 2010). In this particular case, stator core electrical resistances are also included in the electrical circuit (CL). Figure 3 shows the equivalent circuit of the no-run-capacitor single-phase induction motor.

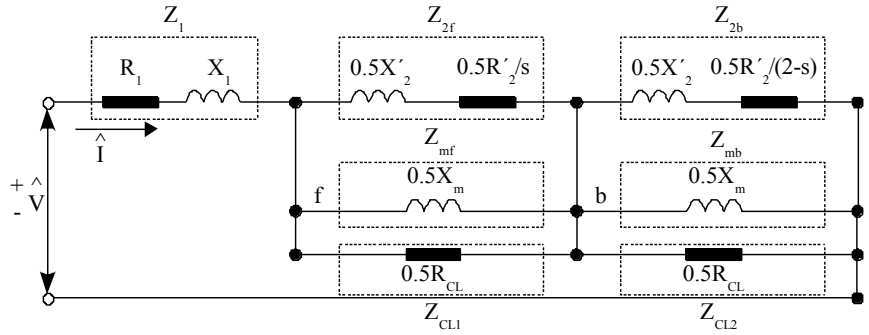

Figure 3. Equivalent circuit of a no-run-capacitor single-phase induction motor.

Rotor and magnetizing parameters are equally divided into forward *(f)* and backward *(b)* rotating magnetic fields, then impedances are modeled according to:

$$Z_1 = R_1 + jX_1; \quad Z_{2f} = 0.5R_2'/s + j0.5X_2'; \quad Z_{mf} = j0.5X_m; \quad Z_{2b} = 0.5R_2'/(2-s) + j0.5X_2';$$
$$Z_{mb} = j0.5X_m; \quad Z_{CL1} = 0.5R_{CL}; \quad Z_{CL2} = 0.5R_{CL} \tag{30}$$

ISSN 2176-5480

where s [-] is the slip ratio, defined as a relation between rotor speed, ω_2 (rad.s^{-1}), and synchronous speed, ω_s (rad.s^{-1}) ($s = 1 - \omega_2/\omega_s$), R'_2 (Ω) is rotor resistance and X'_2 (Ω) is rotor reactance, both referred to the stator side. Magnetizing reactance is X_m (Ω) and stator core resistance is R_{CL} (Ω). The circuit input impedance (Z_{in}) is computed through:

$$Z_{in} = Z_1 + \left(\frac{1}{Z_{2f}} + \frac{1}{Z_{mf}} + \frac{1}{Z_{CL1}}\right)^{-1} + \left(\frac{1}{Z_{2b}} + \frac{1}{Z_{mb}} + \frac{1}{Z_{CL2}}\right)^{-1} \tag{31}$$

where second and third right hand terms are denoted by equivalent impedances Z_f and Z_b, respectively. Z_{in} is used to calculate the input rms current, $\hat{I}$ (A):

$$\hat{I} = \frac{\hat{V}}{Z_{in}} \tag{32}$$

where $\hat{V}$ (V) is rms input voltage. Since voltage drop is unique across impedances Z_f, Z_{2f} and Z_{CL1} and also across impedances Z_b, Z_{2b} and Z_{CL2}, current fluxes at rotor forward and backward branches as well as at stator core are given by:

$$\hat{I}_{2f} = \frac{\hat{I}Z_f}{Z_{2f}}; \qquad \hat{I}_{2b} = \frac{\hat{I}Z_b}{Z_{2b}}; \qquad \hat{I}_{CL1} = \frac{\hat{I}Z_f}{Z_{CL1}}; \qquad \hat{I}_{CL2} = \frac{\hat{I}Z_b}{Z_{CL2}} \tag{33}$$

then all necessary current fluxes are determined.

Electromagnetic losses are due to rotor winding losses and stator winding and core losses. According to Huai *et al.* (2003), those losses account for 75-90% of motor overall losses. Therefore, input losses to the current thermal model are based on these electromagnetic losses. Stator winding loss depends on the stator winding current and is given by:

$$P_1 = \hat{I}^2 R_1 \tag{34}$$

whereas forward and backward powers arise from the rotating magnetic fields:

$$P_{2f} = \hat{I}_{2f}^2 \frac{0.5R_2^{'}}{s}; \qquad P_{2b} = \hat{I}_{2b}^2 \frac{0.5R_2^{'}}{2-s} \tag{35}$$

and rotor winding loss (P_2) is computed as a combination of the forward and backward power components:

$$P_2 = sP_{2f} + (2-s)P_{2b} \tag{36}$$

Finally, stator core losses are calculated as a sum of contributions in CL1 and CL2 branches:

$$P_{CL} = 0.5R_{CL}\left(\hat{I}_{CL1}^2 + \hat{I}_{CL2}^2\right) \tag{37}$$

The rate of energy that is not converted into heat is the shaft power, P_{mec} (W), and is given by the difference between the forward and backward rotating fields powers:

$$P_{mec} = (1-s)\left(P_{2f} - P_{2b}\right) \tag{38}$$

Indeed, P_{mec} is the useful power delivered to the crankshaft and matches the system requirement, represented by the power to compress the gas, P_{ind} (W), and by bearings friction losses, P_{bea} (W), ($P_{mec} = P_{ind} + P_{bea}$). P_{ind} is estimated from an ideal isentropic compression process and friction losses at compressor suction and discharge systems, which are usually around 10% of the isentropic power, i.e.:

$$P_{ind} = 1.1\dot{m}\frac{p_e}{\rho_s}\frac{k}{k-1}\left[\left(\frac{p_c}{p_e}\right)^{\frac{k-1}{k}} - 1\right] \tag{39}$$

where $\dot{m}$ (kg.s^{-1}) is the refrigerant gas mass flow rate, p_e (Pa) and p_c (Pa) are evaporating and condensing pressures, respectively, ρ_s (kg.m^{-3}) is the refrigerant gas density in the compressor suction system and k (-) is an isentropic coefficient, given by the relation between pressure constant and volume constant specific heats $\left(k = c_p/c_v\right)$. The mass flow rate is obtained from experimental data and remaining parameters from refrigerant gas thermodynamic tables.

ISSN 2176-5480

Based on data from the manufacturer, bearings friction losses, P_{bea}, are estimated to be approximately 9 W and to be almost insensitive in relation to the operating condition. Since the compressor power requirement is computed, the slip ratio is determined in an iterative manner, as described by the algorithm represented in Fig. 4. Finally, electromagnetic losses are obtained and used as input to the thermal model.

Further the aforementioned calculations, an additional verification is carried out. The compressor input power is computed in the electrical model using the following expression:

$$P_{in} = \hat{V}\hat{I}\cos\varphi \tag{40}$$

where φ (º) is the phase angle between input voltage and current and is obtained as the angular component of the polar coordinate representation of Z_{in}. The calculated input power is compared to measurements as an additional check of the electrical model.

4. BOUNDARY CONDITIONS AND PROGRAM EXECUTION

The boundary conditions for the thermal model are measured temperatures in the vicinity of the induction motor, such as in: lubricant oil in carter (3), crankcase (1), refrigerant gas in the motor surrounding (2) and compressor shell (27). Additionally, the heat generation in stator windings (41, 42 and 43), rotor windings (11, 15, 17 and 19) and stator core (25) are input to the thermal model.

The electrical model requires a set of resistance and reactance values, as observed in Fig. 3. Since electrical resistance of rotor and stator windings depend on temperature, such a data is an input to the electrical model. The relation between those parameters is given by:

$$R = R_0 + \alpha R_0 (T - T_0) \tag{41}$$

where subscript *0* refers to the reference state and α (K^{-1}) is the temperature coefficient, which is a property of the material. All the electrical parameters were supplied by the manufacturer. As long as all boundary conditions are stated, the computational program is executed following the algorithm described in Fig. 4.

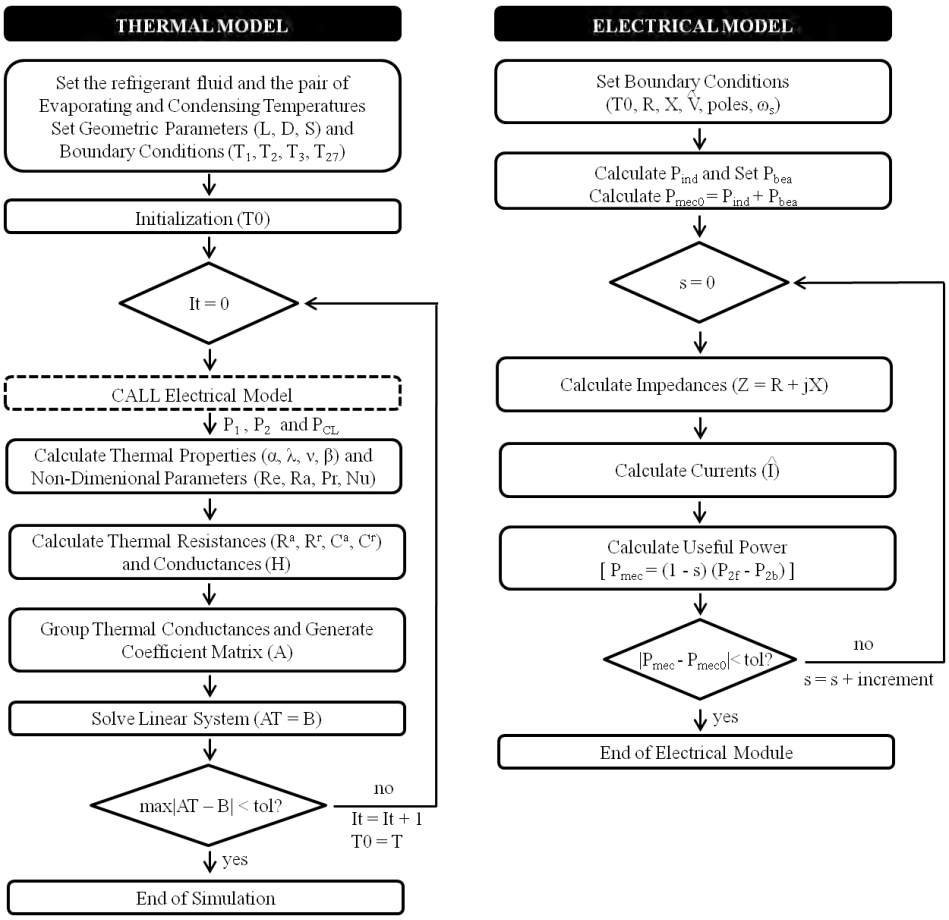

Figure 4. Thermo-electrical model algorithm.

ISSN 2176-5480

5. RESULTS AND DISCUSSIONS

The thermo-electrical model was set using electrical parameters of a given reciprocating compressor and was run under different operating conditions. Table 1 shows the nominal values of the input parameters.

The operating condition (OC) is defined by a set of parameters, such as refrigerant fluid, evaporating and condensing temperatures, gas temperature in the suction line and ambient temperature. In the present work, the compressor is assumed to operate with R290a. Two OCs were evaluated considering different pairs of evaporating and condensing temperatures as well as suction line and ambient temperatures. The OC1 is largely employed in the compressor approval tests and the OC2 is a lower load operating condition established in order to submit the electrical motor to high temperature levels. Experimental data were obtained for both OCs in order to provide boundary conditions and temperature values to validate the numerical results.

Results of rotor and stator temperatures, electromagnetic losses, slip factor, input power and motor efficiency ($\eta = P_{mec}/P_{in}$) are shown in Tab. 2. Since measurements of temperature were not carried out in the rotor due to instrumentation difficulties, experimental data are available only for stator regions. It should be mentioned that the numerical results for rotor temperatures in Tab. 2 are averages in the associated component. For example, the temperature of the rotor ring was taken as an arithmetic average of the temperatures calculated for the rings 17 and 19. Such an average procedure was not adopted for the stator temperatures, since very small temperature variations occurred in the stator. Experimental data for temperature are also averaged values of thermocouple readings in different parts of each component.

Table 1.Compressor electrical parameters - nominal values.

Input Voltage (V)	220
Synchronous Frequency (Hz)	50
Number of Poles (-)	2
Stator Main Winding Resistance (Ω) at 25ºC	11.6
Stator Main Winding Leakage Reactance (Ω)	16.2
Rotor Winding Resistance - referred to stator side (Ω) at 25ºC	11.0
Rotor Leakage Reactance - referred to stator side (Ω)	4.5
Magnetizing Reactance (Ω)	857
Stator Iron Resistance (Ω) at 25ºC	10,000

Table 2. Numerical and experimental results.

	OC1: -23.3ºC/54.4ºC $T_{suctionline}$: 32ºC $T_{ambient}$: 32ºC			**OC2: -35.0ºC/70.0ºC $T_{suctionline}$: 40ºC $T_{ambient}$: 43ºC**		
	Exp.	Num.	Δ	Exp.	Num.	Δ
$T_{statorcoil}$(ºC) 42	80.0	81.3	-1.4	93.1	95.4	-2.2
$T_{statorslot}$ (ºC) 41	80.1	81.6	-1.5	92.8	95.7	-2.9
$T_{statorcore}$(ºC) 25	78.5	81.9	-3.4	92.9	96.0	-3.1
$T_{rotorring}$(ºC) av. 17, 19	-	76.7	-	-	87.9	-
$T_{rotorbars}$(ºC) av. 11, 15	-	76.6	-	-	87.9	-
$T_{rotorcore}$(ºC) av. 7, 18	-	76.4	-	-	87.7	-
P_1 (W)	-	10.0	-	-	6.9	-
P_2 (W)	-	7.5	-	-	4.6	-
P_{CL} (W)	-	15.9	-	-	16.4	-
s (%)	-	2.2	-	-	1.5	-
P_{in} (W)	150.5	151.5	-1.0	110.1	108.5	1.6
η(%)	-	83.2	-	-	81.9	-

Table 2 shows that predicted temperatures are in agreement with measurements, with deviations being lower than 4ºC. Yet, numerical predictions are higher than experimental data for all stator components, especially the stator core. This disagreement probably occurs because the stator core surface is covered by a thin oil film flow and, hence, the thermocouples there measure the average temperature between the stator core and the oil film. Since the oil film flow over the stator core is not taken into account in the thermal model, the temperatures predicted for the stator core and windings (coils and slots) should be expected to be higher than the measurements.

The input power decreases when the operating condition is changed from OC1 to OC2 and this is well predicted by the numerical model. Such a decrease is due to the reduction of the shaft power required by the compressor. Therefore,

ISSN 2176-5480

the current fluxes are expected to become lower in the stator and rotor windings and the same occurring with electromagnetic losses P_1 and P_2. However, motor temperature rises as a whole because the motor efficiency is decreased and the surrounding temperatures are increased. The surrounding temperatures are the boundary conditions of the thermal model and are affected by all compressor losses, including motor, bearings and thermodynamic losses.

Although reasonable agreement between experimental and numerical results is observed, the present motor thermo-electrical model is in an initial stage of development. Further work will be focused on the coupling between the compressor thermodynamic model and the motor thermo-electrical model. Additionally, the electrical model will also be extended to single-phase run-capacitor motors.

6. CONCLUSIONS

This paper presented a simplified methodology to predict the temperature distribution in induction motors of reciprocating compressors commonly adopted for household refrigeration. A thermo-electrical model was developed to this purpose. The thermal model was based in a lumped-parameter formulation with convection boundary conditions prescribed from correlations available in literature. The electrical model adopted the theory of equivalent circuit methodology and used input electrical parameters supplied by the manufacturer. Results were obtained for two operating conditions and compared to experimental data, providing reasonable agreement.

7. ACKNOWLEDGEMENTS

The material discussed herein forms part of a joint technical-scientific program of the Federal University of Santa Catarina and EMBRACO. The authors also acknowledge the support provided by EMBRACO and CNPq (Brazilian Research Council) through Grant No. 573581/2008-8 (National Institute of Science and Technology in Refrigeration and Thermophysics).

8. REFERENCES

Bivari, Y. V.,Gosavi, S. S.,Jorwekar, P. P., 2006. "Use of CFD in design and development of R404a reciprocating compressor." *Proceedings of the International Compressor Engineering Conference at Purdue*, West Lafayette, IN, USA.

Bouafia, M., Ziouchi, A., Bertin, Y. Saulner, J. B., 1999. "Experimental and numerical study of heat transfer in an annular gap without axial flow with a rotating inner cylinder." *International Journal of Thermal Sciences*, Vol. 38, p. 547-559.

Chowdhury, S. K., 2005. "A distributed parameter thermal model for induction motors." In *Proceedings of the International Conference on Power Electronics and Drives Systems - PEDS2005*. Kuala Lumpur, Malaysia.

Churchill, S. W., Chu, H. H. S., 1975. "Correlating equations for laminar and turbulent free convection from a horizontal cylinder." *International Journal of Heat and Mass Transfer*, Vol. 18,p. 1323- 1329.

Cobb, E. C., Saunders, O.A., 1959. "Heat transfer from a rotating disc." In *Proceedings of the Royal Society of London*, Ser. A, Nº 236, p. 343 - 351.

Eltom, A. H., Moharari, N. S., 1991. "Motor temperature estimation incorporating dynamic rotor impedance." *IEEE Transactions on Energy Conversion*, Vol. 6, Nº 1, March 1991, pp. 107 – 113.

Eme, A., Glises, R., Chamagne, D., Kauffmann, J. M., Chalon, F., Péra, T., 2006. "Thermal modelling for electrical machines fed with low voltage first approach of a reliability model." *Mathematics and Computers in Simulation,* Vol. 71, pp. 440-445.

Hrabovcova, V., Kalamen, L., Sekerak, P., Rafajdus, P.,2010. "Determination of single phase induction motors parameters." In *Proceedings of the International Symposium on Power Electronics, Electrical Drives, Automation and Motion - SPEEDAM2010*. Pisa, Italy.

Huai, Y. T., Melnik, R. V. N., Thogersen, P. B., 2003. "Computational analysis of temperature rise phenomena in electric induction motors." *Applied Thermal Engineering,* Vol. 23, pp. 779-795.

Hwang, C. C., Wu, S. S., Jiang, Y. H., 2000. "Novel approach to the solution of temperature distribution in the stator of an induction motor." *IEEE Transactions on Energy Conversion*, Vol. 15, Nº 4, December 2000, pp. 401 – 406.

Incropera, F. P.; Dewitt, D. P., 2011. *Fundamentals of heat and mass transfer.* John Wiley & Sons Inc, USA, 7th edition.

Janssen, L. A. M., Hoogendoorn, C. J., 1978. "Laminar convective heat transfer in helical coiled tubes." *International Heat Mass Transfer,* Vol. 21, pp. 1197-1206.

Mellor, P. H., Roberts, D., Turner, D. R., 1991. "Lumped parameter thermal model for electrical machines of TEFC design." *IEEE Proceedings-B*, Vol. 138, Nº 5, September 1991, pp. 205 – 218.

Mezani, S., Takorabet, N., Laporte, B. "A combined electromagnetic and thermal analysis of induction motors." *IEEE Transactions on Magnetics*, Vol. 41, Nº 5, May 2005, pp. 1572 – 1575.

ISSN 2176-5480

Ooi, K. T., 2003. "Heat transfer study of a hermetic refrigeration compressor." *Applied Thermal Engineering,* Vol. 23, pp. 1931-1945.

Padhy, S.K., 1992. "Heat transfer model of a rotary compressor." *Proceedings of the International Compressor Engineering Conference at Purdue*, West Lafayette, IN, USA.

Raja, B., Sekhar, S. J., Lal, D. M., Kalanidhi, A., 2003. "A numerical model for thermal mapping in a hermetically sealed reciprocating compressor." *International Journal of Refrigeration*, Vol. 26, pp. 652-658.

Rajagopal, M. S., Seetharamu, K. N., Ashwathnarayana, P. A., 1998. "Transient thermal analysis of induction motors." *IEEE Transactions on Energy Conversion*, Vol. 13, Nº 1, March 1998, pp. 62 – 69.

Sanvezzo Jr., J., Deschamps, C. J., 2012. "A heat transfer model combining differential and integral formulations for thermal analysis of reciprocating compressors." *Proceedings of the International Compressor Engineering Conference at Purdue*, West Lafayette, IN, USA.

Sarkar, D, Naskar, A. K., 2012. "Approximate analysis of 2-dimensional heat conduction in the rotor of an induction motor during reactor starting." In *Proceedings of IEE 5th India International Conference on Power Electronics*. Delhi, India.

Schreiner, J. E., 2008. *Desenvolvimento de metodologias de simulação para análise de soluções de gerenciamento térmico aplicadas a compressores alternativos de refrigeração.* Master's thesis, Federal University of Santa Catarina, Florianopolis, Brazil.

Todescat, M. L., Fagotti, F., Ferreira R. T. S., Prata, A. T., 1992. "Thermal energy analysis in reciprocating hermetic compressors." *Proceedings of the International Compressor Engineering Conference at Purdue*, West Lafayette, IN, USA.

Umans, S. D., 1996. "Steady-state, lumped-parameter model for capacitor-run, single-phase induction motors." *IEEE Transactions on Industry Applications*, Vol. 32, Nº 1, January/February 1996, pp. 169 – 179.

Voigdlener, T., 2004. *Escoamento e transferência de calor em motores elétricos de indução.* Master's thesis, Federal University of Santa Catarina, Florianopolis, Brazil.

Whitaker, S., 1972. "Forced convection heat transfer correlations for flow in pipes, past flat plates, single cylinders, single spheres, and flow in packed beds and tube bundles." *American Institute of Chemical Engineers Journal*, Vol. 18, p. 361-371.

9. RESPONSIBILITY NOTICE

The authors are the only responsible for the printed material included in this paper.